

Synthesis and Characterization of Bis(S-acetylthio)-Derivatized Europium Triple-Decker Monomers and Oligomers

Karl-Heinz Schweikart,[†] Vladimir L. Malinovskii,[†] Amir A. Yasseri,[‡] Junzhong Li,[†] Andrey B. Lysenko,[†] David F. Bocian,^{*†} and Jonathan S. Lindsey^{*†}

Departments of Chemistry, North Carolina State University, Raleigh, North Carolina 27695-8240, and University of California, Riverside, California 92521-0403

Received June 26, 2003

We report the synthesis of monomers, dimers, trimers, and oligomers of triple-decker (TD) complexes bearing S-acetylthio groups at the termini: AcS-(TD)_n-SAc. Each TD was of type (Pc)Eu(Pc)Eu(Por), where H₂Pc = tetra-*tert*-butylphthalocyanine and H₂Por is a *meso*-tetraarylporphyrin bearing functional groups at the 4-aryl position such as ethynyl, TMS-ethynyl, TIPS-ethynyl, or iodo. The TD arrays were prepared by Sonogashira- and Glaser-type coupling reactions, affording 1,4-diphenylethyne or 1,4-diphenylbutadiyne linkers joining the TDs. Each TD array exhibited high solubility in organic solvents such as CHCl₃ or CH₂Cl₂. Self-assembled monolayers (SAMs) of all the TDs were prepared on Au substrates and investigated via a variety of electrochemical techniques aimed at determining redox potentials, rates of electron transfer under applied potential, and rates of charge retention in the absence of applied potential. The electrochemical measurements were accompanied by ellipsometric studies aimed at determining SAM thickness and, hence, the orientation of the complexes with respect to the surface plane. All of the TD SAMs exhibit robust, reversible voltammetry yielding four well-resolved waves in the potential range of 0 to +1.6 V (corresponding to the mono-, di-, tri-, and tetracations). The electron-transfer rates for the various oxidation states of all of the TD SAMs are similar and in the 10⁴–10⁵ s⁻¹ range. The charge-dissipation rates (measured in terms of a charge-retention half-life) are also similar and are in the 10–60 s range. These rates are influenced by both the packing density of the molecules and the orientation of the molecules on the surface. The full body of data supports the view that all of the dithio-derivatized TD complexes assume a similar geometry on the surface. In particular, the complexes are oriented with their linkers/macrocycle planes generally parallel with the surface, unlike monothio-derivatized analogues, which are in a more perpendicular geometry. The parallel geometry of the dithio-derivatized TDs is qualitatively consistent with covalent attachment to Au via both thiols.

Introduction

In a series of earlier studies, we have demonstrated that porphyrinic molecules attached to electroactive surfaces can store charge for significant periods of time upon disconnection from the source of applied potential.^{1–6} This character-

istic renders these materials excellent candidates to function as molecular capacitors in next-generation information storage media. Among the various classes of porphyrinic molecules that we have examined, the triple-decker (TD) sandwich complexes comprised of porphyrin and phthalocyanine ligands and lanthanide metals exhibit some of the most desirable properties for information-storage applications.^{5,7,8} In par-

* To whom correspondence should be addressed. E-mail: jlindsey@ncsu.edu (J.S.L.); David.Bocian@ucr.edu (D.F.B.).

[†] North Carolina State University.

[‡] University of California.

- (1) Roth, K. M.; Dontha, N. R.; Dabke, B.; Gryko, D. T.; Clausen, C.; Lindsey, J. S.; Bocian, D. F.; Kuhr, W. G. *J. Vac. Sci. Technol., B* **2000**, *18*, 2359–2364.
- (2) Roth, K. M.; Liu, Z.; Gryko, D. T.; Clausen, C.; Lindsey, J. S.; Bocian, D. F.; Kuhr, W. G. *ACS Symp. Ser.* **2003**, *844*, 51–61.
- (3) Roth, K. M.; Lindsey, J. S.; Bocian, D. F.; Kuhr, W. G. *Langmuir* **2002**, *18*, 4030–4040.
- (4) Roth, K. M.; Gryko, D. T.; Clausen, C.; Li, J.; Lindsey, J. S.; Kuhr, W. G.; Bocian, D. F. *J. Phys. Chem. B* **2002**, *106*, 8639–8648.

- (5) Gryko, D.; Li, J.; Diers, J. R.; Roth, K. M.; Bocian, D. F.; Kuhr, W. G.; Lindsey, J. S. *J. Mater. Chem.* **2001**, *11*, 1162–1180.
- (6) Roth, K. M.; Yasseri, A. A.; Liu, Z.; Dabke, R. B.; Malinovskii, V.; Schweikart, K.-H.; Yu, L.; Tiznado, H.; Zaera, F.; Lindsey, J. S.; Kuhr, W. G.; Bocian, D. F. *J. Am. Chem. Soc.* **2003**, *125*, 505–517.
- (7) Li, J.; Gryko, D.; Dabke, R. B.; Diers, J. R.; Bocian, D. F.; Kuhr, W. G.; Lindsey, J. S. *J. Org. Chem.* **2000**, *65*, 7379–7390.
- (8) Schweikart, K.-H.; Malinovskii, V. L.; Diers, J. R.; Yasseri, A. A.; Bocian, D. F.; Kuhr, W. G.; Lindsey, J. S. *J. Mater. Chem.* **2002**, *12*, 808–828.

ticular, the TDs (1) are very stable species and (2) typically exhibit a large number of accessible oxidation states (as many as nine, ranging from -4 through neutral to $+4$, in a potential range of -1.2 to $+1.6$ V).^{9,10} The availability of multiple oxidation states imparts several advantages to a TD-based molecular capacitor. (1) The amount of charge that can be stored in a particular location is increased, facilitating detection in a reading operation. (2) The relatively low potentials of the redox events would lessen power consumption in an actual device. (3) The discrete voltage steps associated with each redox event afford the possibility of multibit information storage. For practical purposes, we have focused our studies on π -cation-radical TD complexes rather than on π -anions.^{5,7,8} The cations are more amenable to implementation in devices because they are relatively stable under real-world (i.e., oxidizing) conditions. This is not the case for anions, which are highly unstable under oxidizing conditions. The TDs typically exhibit four cationic states in the potential range of 0 to $+1.6$ V, thus enabling the storage of two bits of information.

In the course of our studies of TD complexes, we developed the methodology for the rational synthesis of certain types of TDs,¹¹ for the attachment of thiol linkers to a porphyrin constituent in the TD complex,^{5,7} and for the preparation of dyads of thiol-derivatized TDs.⁸ We have shown that all of the thiol-derivatized TDs form self-assembled monolayers (SAMs) on Au surfaces and exhibit robust, reversible electrochemical behavior.^{5,7,8} For selected TD SAMs, we have also measured the electron-transfer rate in the presence of applied potential and the charge-dissipation rate in the absence of applied potential.⁴ The former rate dictates the ultimate speed at which information can be stored and accessed in a molecular capacitor. The latter rate determines how fast the stored charge leaks from the capacitor and thereby how frequently a memory cell based on the molecular capacitor would need to be refreshed.

In the TD dyads that we previously prepared, the constituent TDs were joined via a 4,4'-diphenylethyne group.⁸ In studies of the cations of these TD dyads⁸ and the cations of analogous multiporphyrin arrays,^{12–14} we have found that the 4,4'-diphenylethyne connector affords facile hole/electron migration among the constituents via a superexchange process. Similar results were achieved with arrays joined via a 4,4'-diphenylbutadiyne linker.¹⁵ Hole/electron migration provides a mechanism for moving charge to a site in a surface-attached oligomeric species that is distal to the site of the initial redox event, thereby accessing redox centers far from the electroactive surface.

Our objectives in this work were to prepare and characterize linear oligomers of TDs that are joined via 4,4'-diphenylethyne or 4,4'-diphenylbutadiyne connectors and functionalized for attachment to an electroactive surface. Upon attachment to the surface, each TD constituent should be readily oxidized or reduced upon application of a suitable electrochemical potential. The TD oligomers described herein bear two thio-derivatized linkers, one at each end of the oligomer. We elected to work with *S*-acetylthio groups to avoid handling free thiols;^{16,17} the *S*-acetyl group undergoes facile cleavage upon contact with Au.^{7,16,18–21} While there are a few reports on oligo(1,4-phenyleneethynylene)s bearing thio-ester groups on both ends of the arrays,^{22,23} there are no prior examples in the literature of corresponding oligomers based on TD sandwich complexes. The fact that the oligomers contain thiols at each end affords the ability to address the question of the orientation of the molecules with respect to the surface. In particular, do the oligomers stand in a more upright geometry, which necessitates that attachment is via only one of the two thiols? Or, do the oligomers lie in a more prone orientation, which could occur if attachment is via only one thiol and would be necessitated if attachment is via both thiols? Regardless of which orientation/attachment chemistry is preferred, this characteristic of the oligomers would be important in any type of device that incorporated the molecules.

In the work reported herein, we first describe the synthesis of the monomeric porphyrin and TD building blocks. We then report on the synthesis of bis(*S*-acetylthio)-derivatized TD arrays (monomer, dimer, and trimer as shown in Chart 1) and the polymerization of diethyne-substituted TDs in a Glaser-type coupling reaction.²⁴ We then describe a series of electrochemical studies designed to evaluate the redox characteristics, molecular charge density, and surface coverage of SAMs of the various TDs on Au. We also examine both the electron-transfer and charge-dissipation rates of the TD SAMs. The electrochemical studies are augmented with ellipsometric studies to investigate the SAM thickness, and hence, the molecular orientation on the surface. Collectively, these studies establish a relatively self-consistent picture of the electrochemical and geometrical properties of the TD SAMs.

(9) Duchowski, J. K.; Bocian, D. F. *J. Am. Chem. Soc.* **1990**, *112*, 8807–8811.

(10) Ng, D. K. P.; Jiang, J. *Chem. Soc. Rev.* **1997**, *26*, 433–442.

(11) Gross, T.; Chevalier, F.; Lindsey, J. S. *Inorg. Chem.* **2001**, *40*, 4762–4774.

(12) Seth, J.; Palaniappan, V.; Johnson, T. E.; Prathapan, S.; Lindsey, J. S.; Bocian, D. F. *J. Am. Chem. Soc.* **1994**, *116*, 10578–10592.

(13) Seth, J.; Palaniappan, V.; Wagner, R. W.; Johnson, T. E.; Lindsey, J. S.; Bocian, D. F. *J. Am. Chem. Soc.* **1996**, *118*, 11194–11207.

(14) Holten, D.; Bocian, D. F.; Lindsey, J. S. *Acc. Chem. Res.* **2002**, *35*, 57–69.

(15) Youngblood, W. J.; Gryko, D. T.; Lammi, R. K.; Bocian, D. F.; Holten, D.; Lindsey, J. S. *J. Org. Chem.* **2002**, *67*, 2111–2117.

(16) Tour, J. M.; Jones, L. II; Pearson, D. L.; Lamba, J. J. S.; Burgin, T. P.; Whitesides, G. M.; Allara, D. L.; Parikh, A. N.; Atre, S. V. *J. Am. Chem. Soc.* **1995**, *117*, 9529–9534.

(17) Gryko, D. T.; Clausen, C.; Lindsey, J. S. *J. Org. Chem.* **1999**, *64*, 8635–8647.

(18) Gryko, D. T.; Clausen, C.; Roth, K. M.; Dontha, N.; Bocian, D. F.; Kuhr, W. G.; Lindsey, J. S. *J. Org. Chem.* **2000**, *65*, 7345–7355.

(19) Gryko, D. T.; Zhao, F.; Yasserli, A. A.; Roth, K. M.; Bocian, D. F.; Kuhr, W. G.; Lindsey, J. S. *J. Org. Chem.* **2000**, *65*, 7356–7362.

(20) Clausen, C.; Gryko, D. T.; Dabke, R. B.; Dontha, N.; Bocian, D. F.; Kuhr, W. G.; Lindsey, J. S. *J. Org. Chem.* **2000**, *65*, 7363–7370.

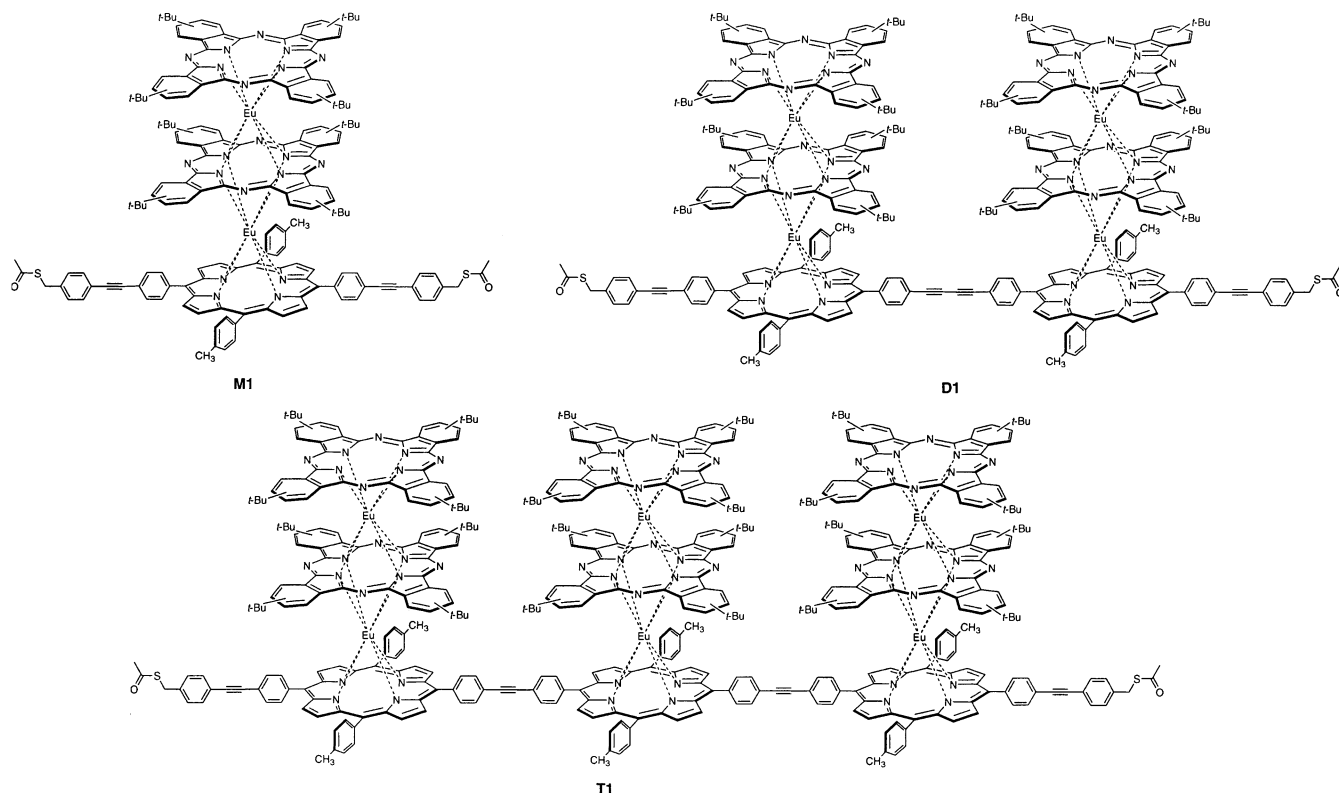
(21) Clausen, C.; Gryko, D. T.; Yasserli, A. A.; Diers, J. R.; Bocian, D. F.; Kuhr, W. G.; Lindsey, J. S. *J. Org. Chem.* **2000**, *65*, 7371–7378.

(22) Pearson, D. L.; Tour, J. M. *J. Org. Chem.* **1997**, *62*, 1376–1387.

(23) Jones, L. II; Schumm, J. S.; Tour, J. M. *J. Org. Chem.* **1997**, *62*, 1388–1410.

(24) Liu, Q.; Burton, D. J. *Tetrahedron Lett.* **1997**, *38*, 4371–4374.

Chart 1



Results

1. Synthesis of the Bis(*S*-acetylthio)-Derivatized TD Complexes. Strategy. TD sandwich complexes have been prepared of form (Por)Ln(Pc)Ln(Por) (type a), (Pc)Ln(Por)-Ln(Pc) (type b), and (Pc)Ln(Pc)Ln(Por) (type c), where Ln = lanthanide, H₂Pc is a phthalocyanine, and H₂Por is a porphyrin.^{5,10} We recently developed methodology to synthesize type c TDs in a rational manner (extending the Weiss procedure²⁵) by reaction of a europium phthalocyanine double-decker complex with a europium porphyrin half-sandwich complex.¹¹ The latter is formed in situ from Eu(acac)₃·*n*H₂O and the free-base porphyrin in refluxing 1,2,4-trichlorobenzene.^{11,26} Accordingly, we have employed type c TDs in this application. Synthetic handles in the TDs are incorporated via a suitably functionalized porphyrin rather than a phthalocyanine, because the synthetic chemistry of the former is better developed.²⁷ Iodophenyl and ethynylphenyl groups attached to the porphyrin constitute suitable handles for Sonogashira- or Glaser-type coupling of thio-derivatized linker groups at the TD stage or coupling of the TDs to give linear arrays.

Functionalized Porphyrin Monomers. Two series of porphyrins of types *trans*-A₂B₂ and *trans*-AB₂C have been prepared bearing iodo and/or trimethylsilyl (TMS) or triisopropylsilyl (TIPS) protected ethyne groups. The syntheses

begin with dipyrromethanes **1–5**, which have been prepared previously via a one-flask reaction of an aldehyde with excess pyrrole.^{28–32} The synthesis of *trans*-A₂B₂-porphyrins is readily achieved by the self-condensation of a dipyrromethane monocarbinol.³⁰ The *trans*-AB₂C-porphyrins are prepared by condensation of a dipyrromethane dicarbinol and a dipyrromethane.³² Both porphyrin-forming procedures are rational and proceed under mild conditions.

Following a general procedure,³² reaction of a dipyrromethane (**1–3**) with a pyridyl thioester (**6–8**)^{30,32} at low temperature gave the monoacylated dipyrromethane (**9–11**) in good yield (Scheme 1). Reduction of **9** with NaBH₄ followed by self-condensation of the resulting carbinol afforded the desired *trans*-A₂B₂ diiodoporphyrin **12** in 31% yield (Scheme 2).

Two approaches for the synthesis of a *trans*-A₂B₂ diethynyl porphyrin are shown in Scheme 3. In one approach, treatment of **11** with *n*-Bu₄NF in THF gave the ethynyl monoacyl dipyrromethane **13** in excellent yield. Reduction of **13** and self-condensation of the resulting carbinol afforded the desired *trans*-A₂B₂ porphyrin **14** in 30% yield. Reduction of **10**³⁰ followed by self-condensation of the resulting monocarbinol under new acid catalysis conditions (InCl₃ in CH₂Cl₂)³³ afforded *trans*-A₂B₂ porphyrin **15** bearing two

(25) Chabach, D.; De Cian, A.; Fischer, J.; Weiss, R.; El Malouli Bibout, M. *Angew. Chem., Int. Ed. Engl.* **1996**, *35*, 898–899.

(26) Wong, C.-P.; Venteicher, R. F.; Horrocks, W. D. Jr. *J. Am. Chem. Soc.* **1974**, *96*, 7149–7150.

(27) Lindsey, J. S. In *The Porphyrin Handbook*; Kadish, K. M., Smith, K. M., Guilard, R., Eds.; Academic Press: San Diego, CA, 2000; Vol. 1, pp 45–118.

(28) Lee, C.-H.; Lindsey, J. S. *Tetrahedron*, **1994**, *50*, 11427–11440.

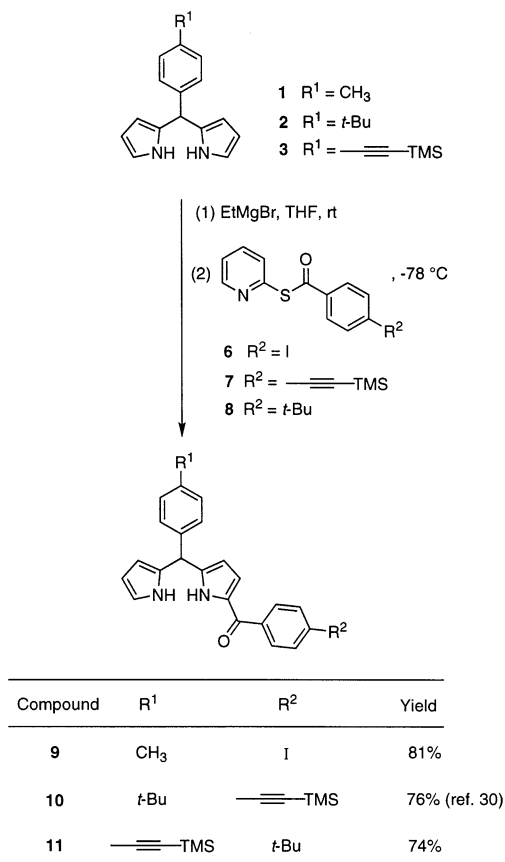
(29) Littler, B. J.; Miller, M. A.; Hung, C.-H.; Wagner, R. W.; O'Shea, D. F.; Boyle, P. D.; Lindsey, J. S. *J. Org. Chem.* **1999**, *64*, 1391–1396.

(30) Rao, P. D.; Littler, B. J.; Geier, G. R., III; Lindsey, J. S. *J. Org. Chem.* **2000**, *65*, 1084–1092.

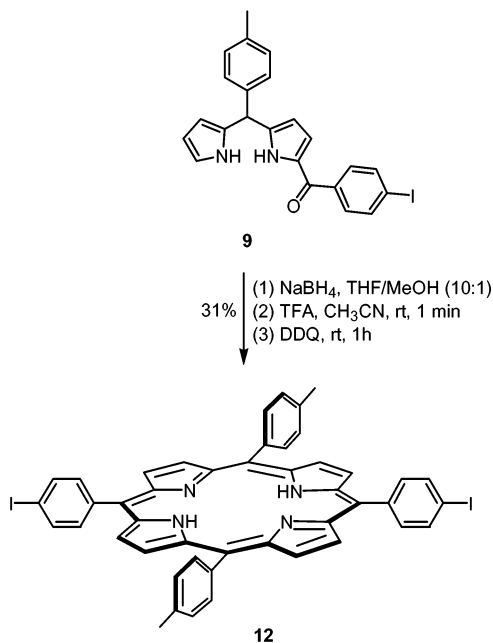
(31) Cho, W.-S.; Kim, H.-J.; Littler, B. J.; Miller, M. A.; Lee, C.-H.; Lindsey, J. S. *J. Org. Chem.* **1999**, *64*, 7890–7901.

(32) Rao, P. D.; Dhanalekshmi, S.; Littler, B. J.; Lindsey, J. S. *J. Org. Chem.* **2000**, *65*, 7323–7344.

Scheme 1



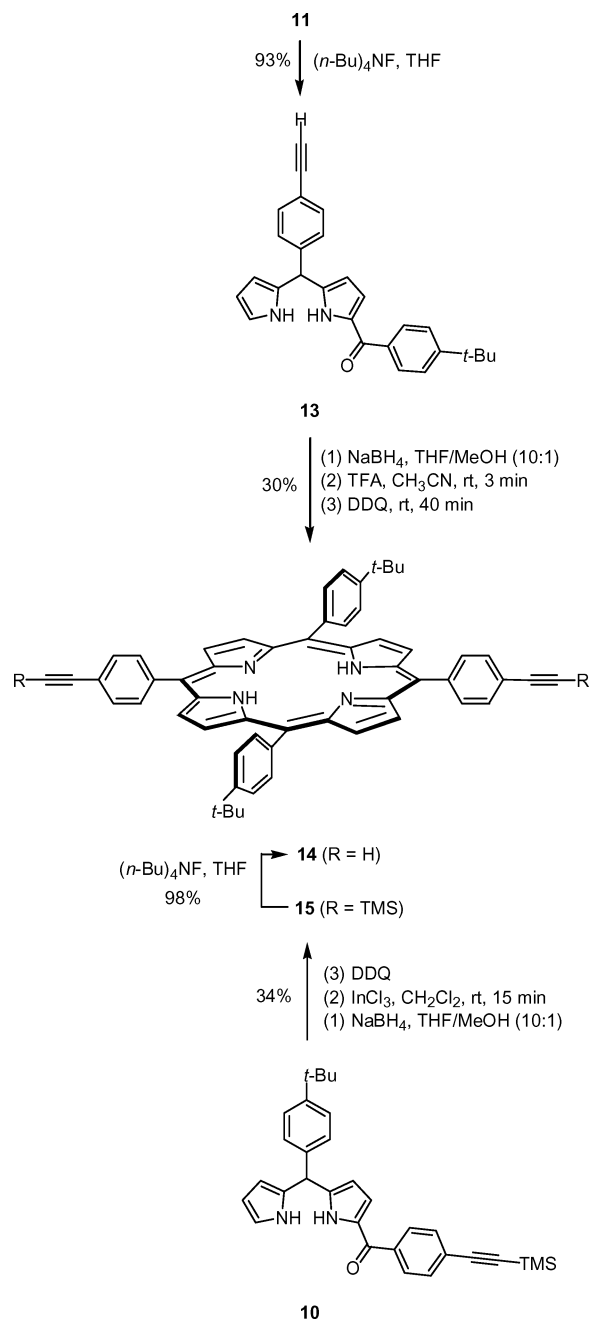
Scheme 2



TMS-protected ethynylphenyl groups in 34% yield (Scheme 3). We did not observe cleavage of the TMS group during porphyrin formation as was noted previously.³⁰ Cleavage of the TMS group with TBAF in THF gave the diethynyl porphyrin **14** in 98% yield.

(33) Geier, G. R., III; Callinan, J. B.; Rao, P. D.; Lindsey, J. S. *J. Porphyrins Phthalocyanines* **2001**, 5, 810–823.

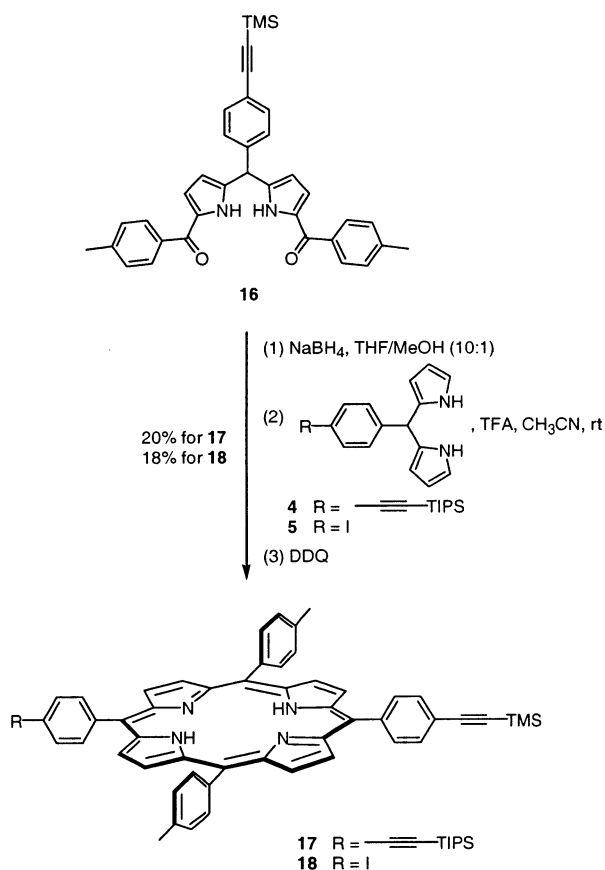
Scheme 3



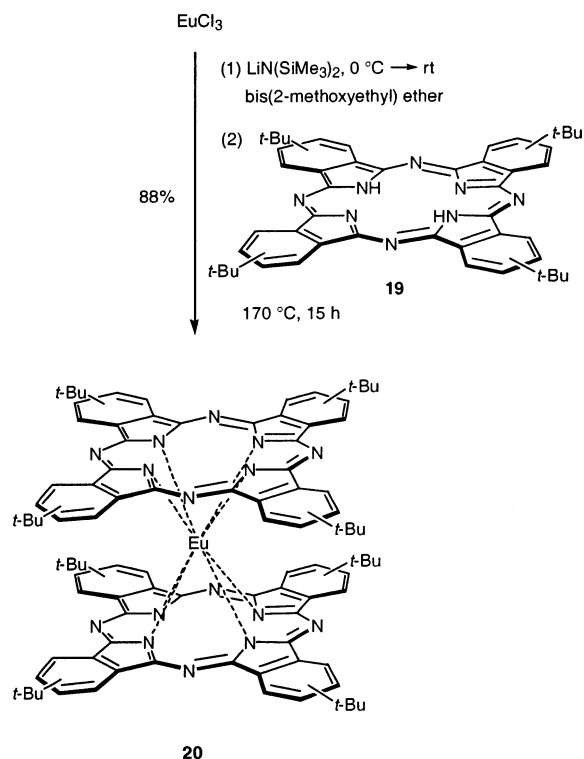
The syntheses of *trans*-AB₂C porphyrins **17** and **18** are shown in Scheme 4. The reduction of **16** with NaBH_4 afforded the dipyrromethane dicarbinol, which upon reaction with dipyrromethane **4** in the presence of TFA (30 mM in acetonitrile) and subsequent oxidation with DDQ at room temperature afforded porphyrin **17** in 20% yield. In the same manner, porphyrin **18**³¹ was resynthesized in 18% yield by treating the dicarbinol of **16** with dipyrromethane **5**.

TD Monomers. The synthesis of the TD monomers of the form (Pc)Eu(Pc)Eu(Por) requires reaction of a porphyrin half-sandwich complex and a phthalocyanine double decker. The synthesis of the phthalocyanine double decker (*t*-Bu₄Pc)₂Eu (**20**) has been reported^{11,34} from the commercially available free-base *t*-Bu₄Pc (**19**) (Scheme 5). The double decker (*t*-Bu₄Pc)₂Eu (**20**) is presumably a radical

Scheme 4

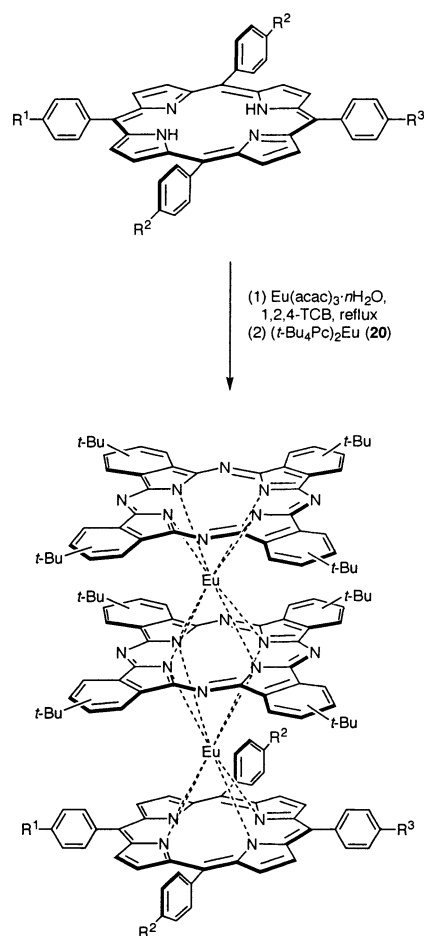


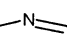




Scheme 5



species.³⁴ Note that **19** and all double-decker and TD complexes based on this phthalocyanine consist of a mixture of (inseparable) regioisomers. We carried out a scaled-up synthesis of double decker **20**, extending the reaction time

Scheme 6



Porphyrin	R ¹	R ²	R ³	TD	Yield
12	I	CH ₃	I	21	69% ^a
14		<i>t</i> -Bu		22	22%
17		CH ₃		23	75% ^a
18	I	CH ₃		24	74% ^b

^a ref. 11 ^b ref. 8

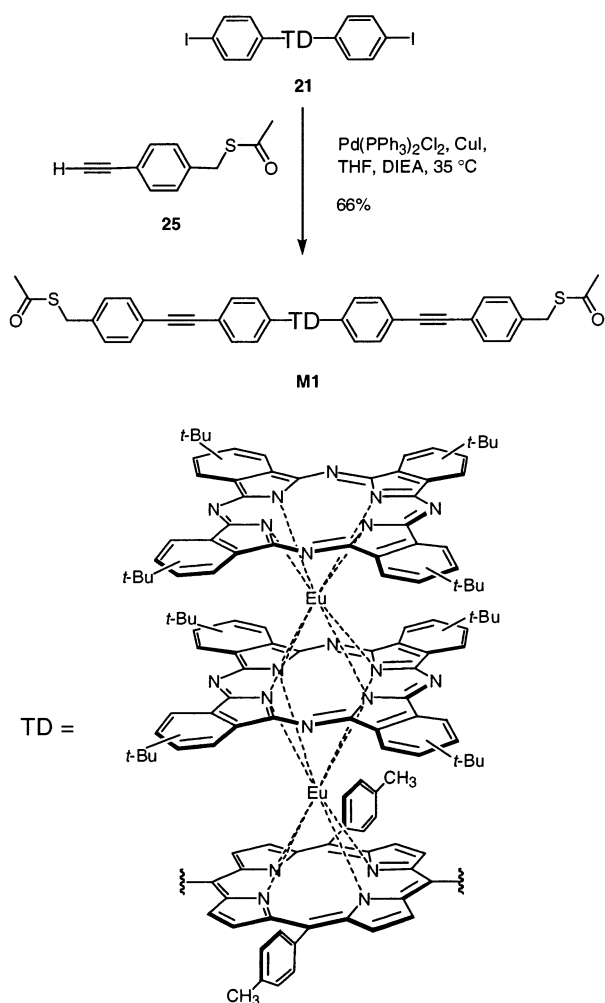
from 4 to 15 h. Purification by size exclusion chromatography (SEC)³⁵ afforded > 500 mg of **20** with a slight improvement in yield (88% versus 78%).

The reaction of porphyrin **12**, **14**, **17**, or **18** with Eu(acac)₃·*n*H₂O gave the corresponding half-sandwich complex. Treatment of the latter with (*t*-Bu₄Pc)₂Eu afforded the TD complex (Scheme 6). TD monomers **21**,¹¹ **23**,¹¹ and **24**⁸ have been prepared previously, while **22** is new.

Bis(S-acetylthio)-Derivatized TD Arrays. The target monomer, dimer, and trimer are shown in Chart 1. Assuming a linear, rodlike orientation, the end-to-end length of monomer **M1** is approximately 35 Å, dimer **D1** is approximately 55 Å, and trimer **T1** is approximately 72 Å. Note that the TD units in **T1** are linked by diphenylethyne groups, whereas a diphenylbutadiyne unit connects the two TDs in dimer **D1**.

(34) Battisti, D.; Tomilova, L.; Aroca, R. *Chem. Mater.* **1992**, *4*, 1323–1328.

Scheme 7

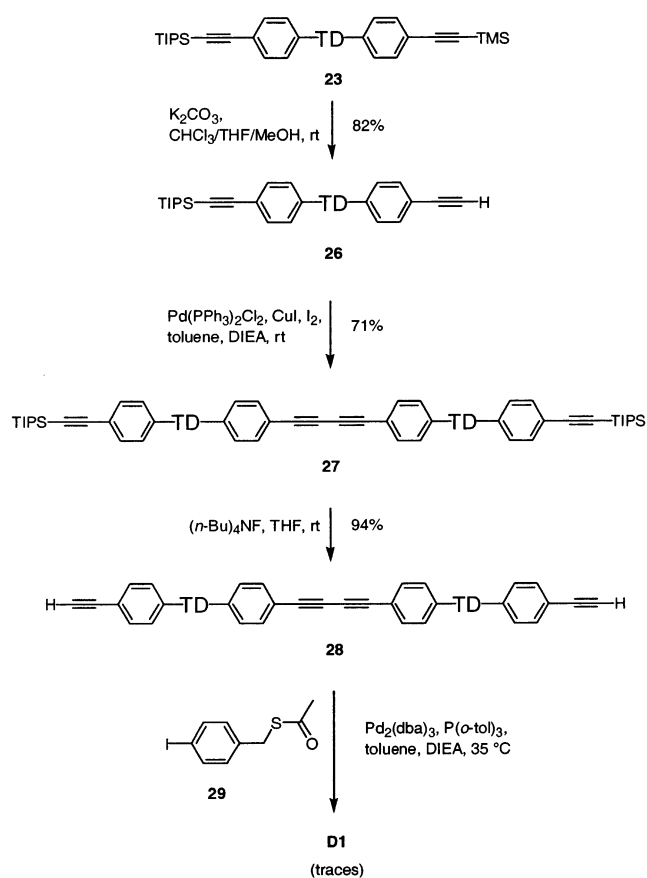


(a) **Monomer.** Sonogashira reaction³⁶ of **21** with 20 equiv of 1-[4-(*S*-acetylthiomethyl)phenyl]ethyne (**25**)¹⁹ in a mixture of THF and *N,N*-diisopropylethylamine (DIEA) containing CuI afforded the target TD molecule **M1** in 66% yield after chromatographic workup (Scheme 7). We chose DIEA rather than other amines to avoid cleavage of the thioester groups;³⁷ however, subsequent work has shown this thioester to be stable to amines such as triethylamine.⁸

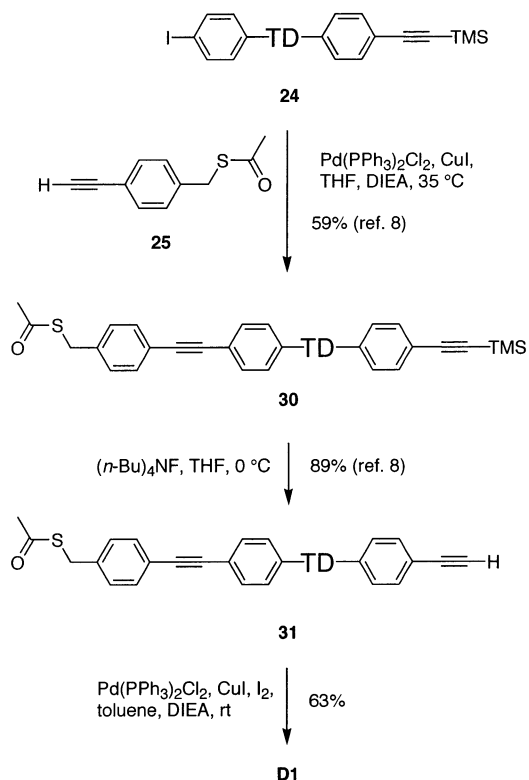
(b) **Dimer.** We investigated the preparation of a dimeric array via two routes: (1) Glaser homocoupling of two ethyne TDs yielding a butadiyne-linked dimer followed by Sonogashira attachment of the two *S*-acetyl linkers (route 1, Scheme 8); (2) Sonogashira attachment of the linker to the monomeric TD followed by Glaser dimerization (route 2, Scheme 9).

Following route 1, the trimethylsilyl (TMS) group of TD **23** was selectively cleaved by treatment with K_2CO_3 at room temperature, affording ethyne TD **26** in 82% yield (Scheme 8). The Glaser-type Pd-catalyzed homocoupling reaction²⁴ of TD **26** gave the corresponding TD dimer **27** in 71% yield

Scheme 8



Scheme 9



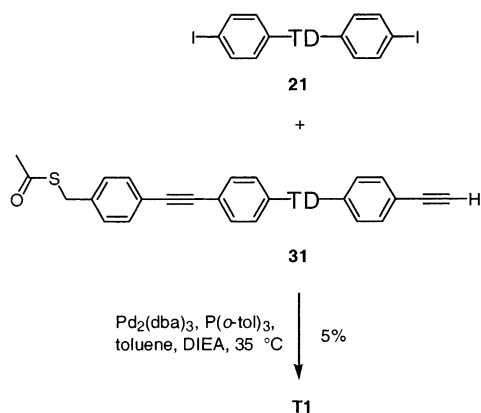
(35) Wagner, R. W.; Johnson, T. E.; Lindsey, J. S. *J. Am. Chem. Soc.* **1996**, *118*, 11166–11180.

(36) Sonogashira, K.; Tohda, Y.; Hagihara, N. *Tetrahedron Lett.* **1975**, 4467–4470.

(37) Hsung, R. P.; Babcock, J. R.; Chidsey, C. E. D.; Sita, L. R. *Tetrahedron Lett.* **1995**, *36*, 4525–4528.

after a three-column procedure.³⁸ The three-column procedure entailed an initial silica column to remove non-TD byproducts, a SEC (THF) column to obtain the desired TD dimer,

Scheme 10



Scheme 11

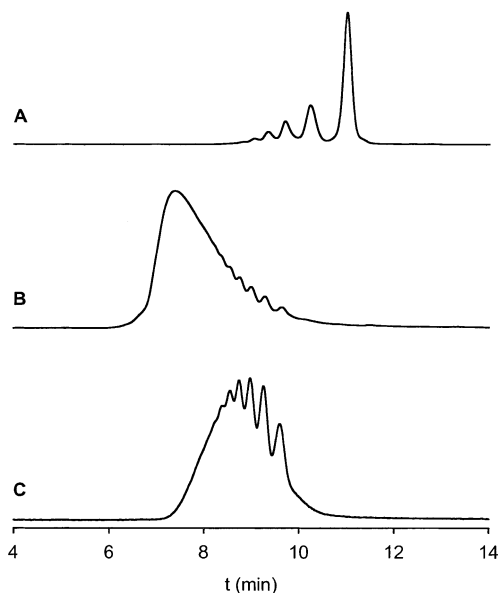
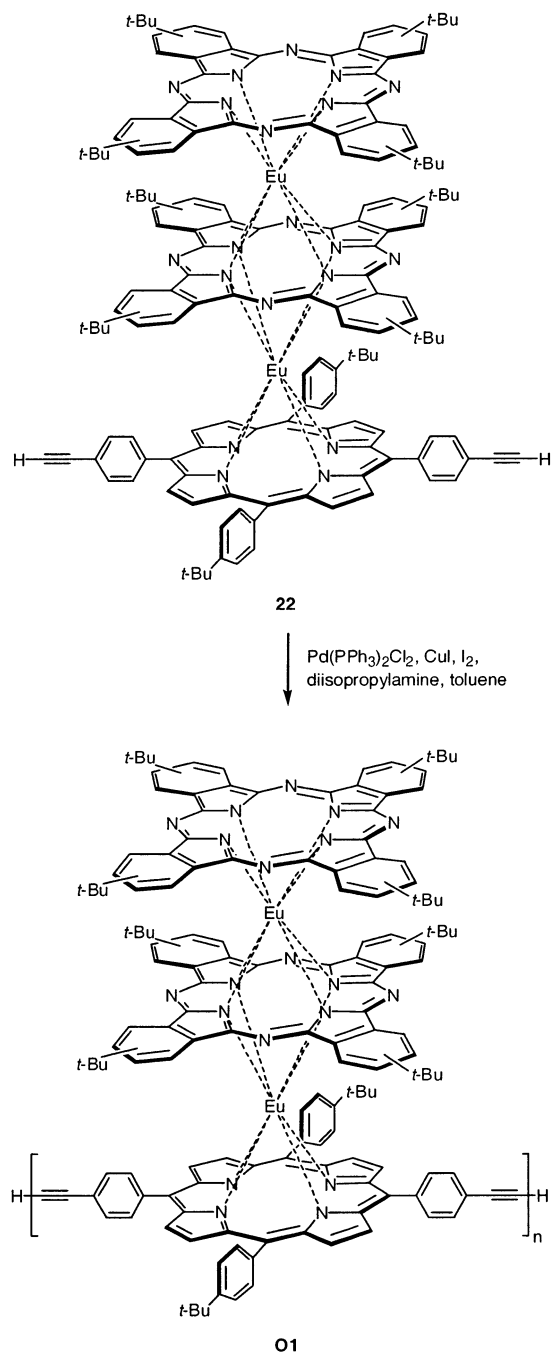


Figure 1. Analytical SEC traces with absorption spectral detection (420 nm, uncorrected for extinction coefficient), obtained with one 1000 Å styrene–divinylbenzene column using THF (0.8 mL/min): (A) crude product distribution (reaction mixture) from the Glaser polymerization of TD monomer **22** after 1 h; (B) mixture of oligomers (**O1**) obtained from the Glaser polymerization of TD monomer **22** (run 1); (C) bis(*S*-acetylthio)-capped mixture of oligomers (**O2**) obtained from polymerization of TD monomer **22** (run 2) followed by addition of the *S*-acetylthio capping unit (**25**).

and a final silica column to remove polar impurities collected from the SEC column. Treatment of dimer **27** with tetrabutylammonium fluoride in THF at room temperature removed the terminal triisopropylsilyl (TIPS) groups, affording ethyne TD dimer **28** in 94% yield.

The reaction of dimer **28** with 1-(*S*-acetylthiomethyl)-4-iodobenzene (**29**)¹⁸ was performed in a mixture of toluene and DIEA (5:1) at 35 °C under copper-free conditions [employing Pd₂(dba)₃ and P(*o*-tol)₃ as the catalyst]³⁹ to avoid the well-known copper-promoted homocoupling of ethynes (yielding butadiyne species). However, a mixture of oligomeric species was obtained as evidenced by analytical SEC. Fractionation (silica, SEC) afforded a trace amount (<1 mg) of the desired product **D1** (*m/z* = 5255.1 upon analysis by laser desorption mass spectrometry, LDMS⁴⁰) together with impurities of higher mass.

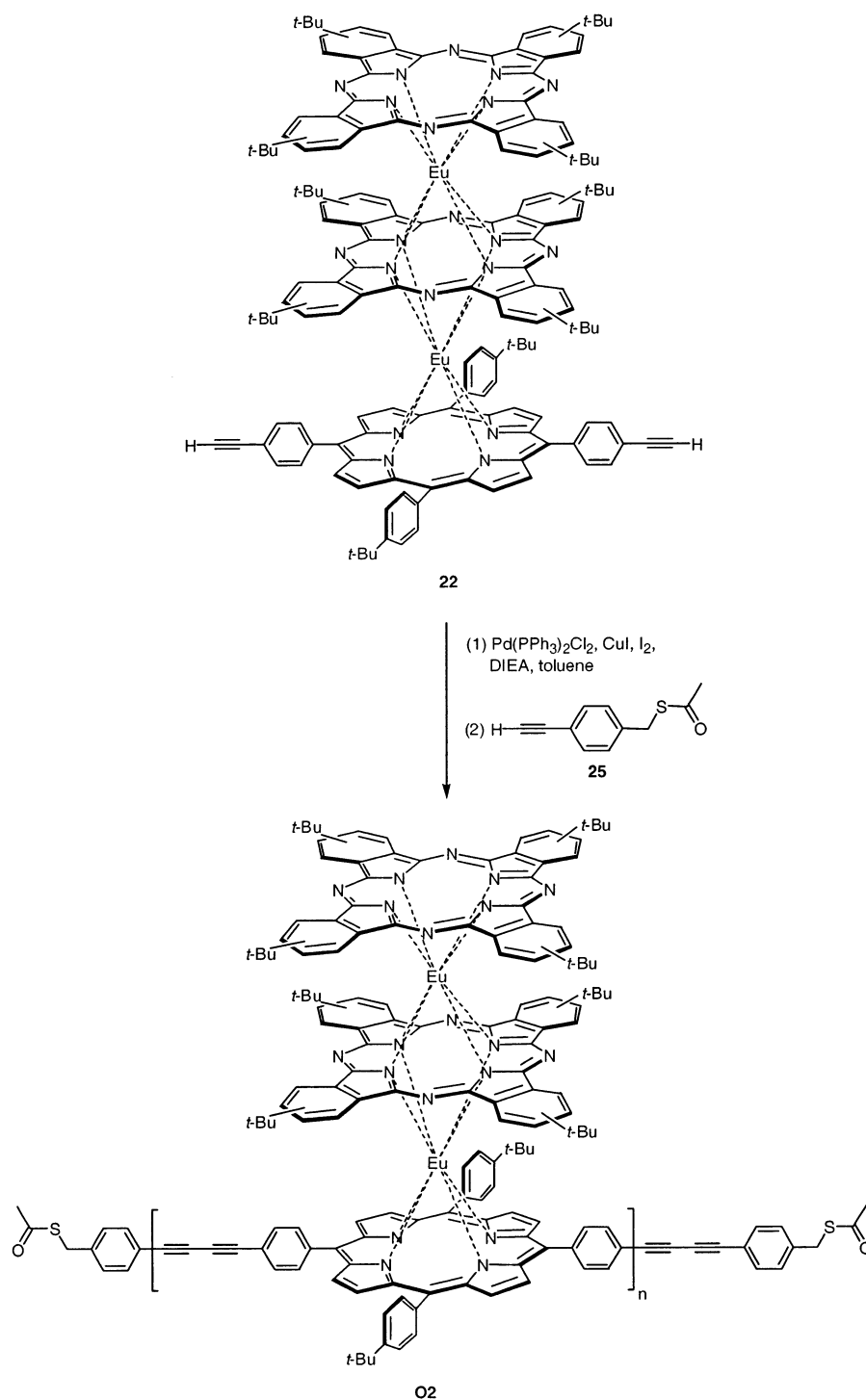
The reverse order of coupling was employed in route 2. Sonogashira coupling of TD **24** with 1-[4-*S*-acetylthiomethyl]phenyl]ethyne (**25**) in the presence of CuI at 35 °C furnished TD **30** in 59% yield after purification by chromatography.⁸ Treatment of **30** with *n*-Bu₄NF in THF at 0 °C for 2 h removed the TMS–ethyne groups, affording **31** in 89% yield.⁸ The Pd-mediated Glaser coupling²⁴ of TD **31** in the presence of CuI and I₂ at room temperature afforded the desired bis(*S*-acetylthio)-derivatized dimer **D1** in 63% yield (19 mg).

(38) Wagner, R. W.; Ciringh, Y.; Clausen, C.; Lindsey, J. S. *Chem. Mater.* **1999**, *11*, 2974–2983.

(39) Wagner, R. W.; Johnson, T. E.; Li, F.; Lindsey, J. S. *J. Org. Chem.* **1995**, *60*, 5266–5273.

(40) Fenyó, D.; Chait, B. T.; Johnson, T. E.; Lindsey, J. S. *J. Porphyrins Phthalocyanines* **1997**, *1*, 93–99.

Scheme 12

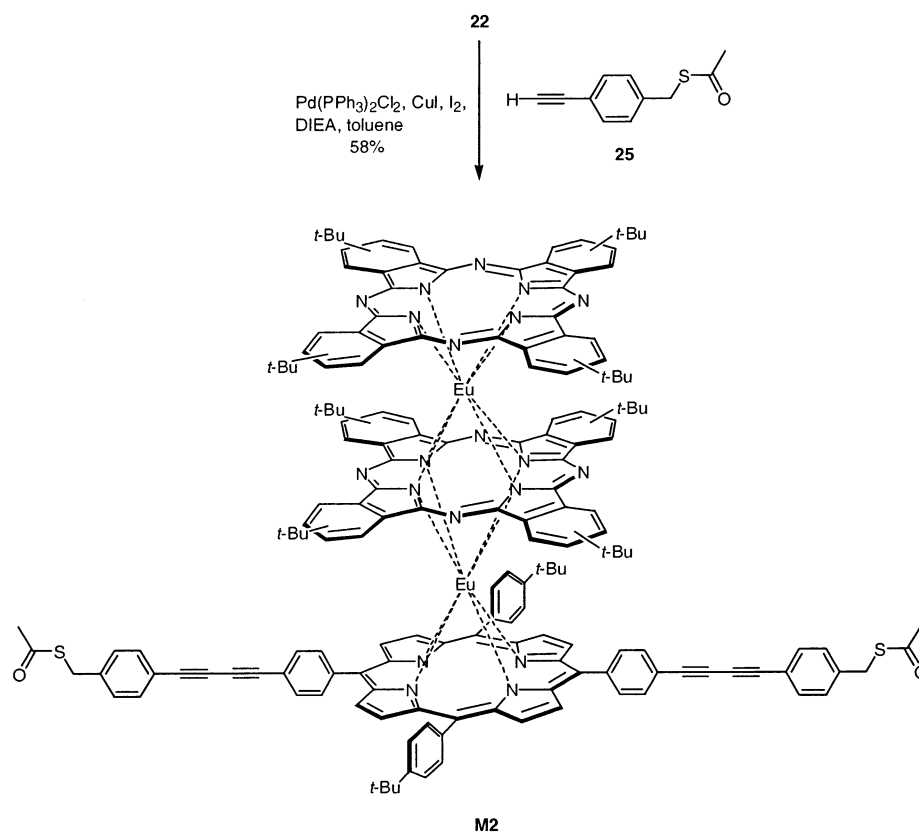


(c) **Trimer.** The *S*-acetyl-derivatized TD **31** was coupled with bis(iodophenyl) TD **21** under the standard copper-free Pd-coupling conditions (to avoid homocoupling of **31**) (Scheme 10). The desired trimer **T1** was obtained in 5% yield after a four-column procedure (silica, SEC, SEC, silica).

(d) **Oligomers.** Our next objective was to investigate the incorporation of TDs into even larger arrays. To address whether oligomeric TD arrays are soluble in organic solvents, the Pd-mediated Glaser coupling of **22** was carried out (Scheme 11). After 1 h, analytical SEC showed distinct peaks corresponding to the starting monomer, a dimer, a trimer, a

tetramer, and a pentamer (Figure 1A). A further batch of Pd catalyst, CuI, and I₂ was added after 4 h. After a total reaction time of 19 h, analytical SEC showed a broad band characteristic of extensive polymerization. After removal of the solvent, the crude product readily dissolved in CHCl₃ and was purified by a three-column procedure to give 5 mg of a green solid. The corresponding SEC trace is shown in Figure 1B. We refer to this product, which is a mixture of oligomers wherein the triple deckers are joined via diphenylbutadiyne linkers and an ethynylphenyl group is located at each terminus, as **O1**. The material was highly soluble in organic

Scheme 13



solvents, auguring well for the use of TD oligomers in diverse applications.

To introduce *S*-acetylthio linkers, TD **22** was polymerized by Glaser coupling (Scheme 12). The reaction was monitored by analytical SEC. After 9 h, excess 1-[4-(*S*-acetylthiomethyl)phenyl]ethyne (**25**) was added to cap the terminal free ethyne groups of the oligomer chains. After 22 h, the reaction mixture was centrifuged. SEC analysis of the supernatant showed no significant change to the product distribution had occurred following the addition of **25**. Purification of the supernatant by SEC (THF) gave two fractions, the first of which contained species from a trimer to higher oligomeric material. The first fraction, designated **O2**, exhibits the SEC chromatogram shown in Figure 1C. The degree of polymerization of **O2** is somewhat lower than that of **O1** (Figure 1B). A second fraction contained mainly dimer and small amounts of a trimer and a tetramer. While mass spectral evidence for end-capping could not be obtained for **O2** owing to the size of the oligomers, MALDI-MS (POPOP) examination of the second fraction showed peaks at $m/z = 5481.5$, 5291.1 , and 5100.5 corresponding to the TD dimer with two, one, and no linker group, respectively. Also, several peaks were found that correspond to fragment ions of these three species. This set of peaks could stem from incomplete coupling or photolysis of a completely coupled product. The presence of at least one *S*-acetylthio end group enables attachment to an Au surface.

The linkers for surface attachment in **O2** are comprised of 4,4'-diphenylbutadiyne units, whereas 4,4'-diphenylethyne groups are employed in TDs **M1**, **D1**, and **T1**. To prepare a

suitable *S*-acetylthio-derivatized TD monomer for comparative studies, compound **22** was reacted with excess **25** (Scheme 13). The linker molecule **25** was employed in excess to minimize self-polymerization of **22** and to completely cap the free ethyne groups of the TD monomer **22**. Monitoring the reaction by analytical SEC showed that only minor amounts of oligomers (a dimer and a trimer) were formed after 3.5 h. After a total reaction time of 22 h and a three-column procedure, bis(*S*-acetylthiomethyl)-substituted TD **M2** was obtained in 58% yield.

2. Physical Properties of the Bis(*S*-acetylthio)-Derivatized TD Complexes. Voltammetric Characteristics of the TDs in Solution and SAMs. The solution electrochemical characteristics of the bis(*S*-acetylthio)-derivatized TDs were examined prior to the studies of the SAMs of these complexes. The solution voltammetric characteristics of all of the TDs are identical; each TD exhibits four distinct anodic waves (not shown) with potentials $E^{0/+} \sim 0.22$ V, $E^{+/+2} \sim 0.57$ V, $E^{+2/+3} \sim 1.08$ V, and $E^{+3/+4} \sim 1.29$ V (vs Ag/Ag⁺; FeCp₂/FeCp₂⁺ = 0.19 V). The observation that the potential for a particular redox wave is approximately the same for each TD is expected because the TDs differ only in the exact nature of the *meso*-aryl substituent groups. The electronic properties of the substituents are not sufficiently different to elicit observable differences in the redox potentials among the complexes (or among inequivalent constituent TDs in the **T1** or **O2** complexes).

Each bis(*S*-acetylthio)-derivatized TD was examined for formation of a SAM on Au microelectrodes. Representative fast scan cyclic voltammograms (100 V s⁻¹) of the **M1** and

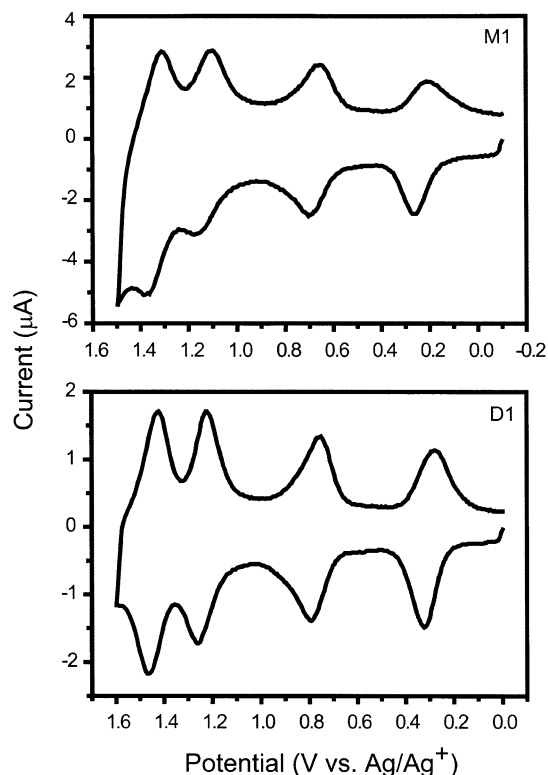


Figure 2. Fast-scan voltammetry (100 V s^{-1}) of the **M1** and **D1** SAMs. The solvent overlayer was CH_2Cl_2 containing $1.0 \text{ M } n\text{-Bu}_4\text{NPF}_6$.

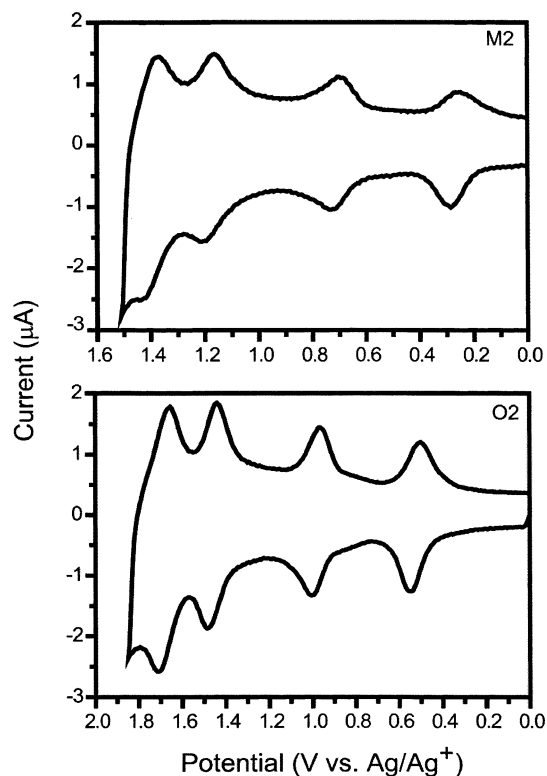


Figure 3. Fast-scan voltammetry (100 V s^{-1}) of the **M2** and **O2** SAMs. The solvent overlayer was CH_2Cl_2 containing $1.0 \text{ M } n\text{-Bu}_4\text{NPF}_6$.

D1 assemblies are shown in Figure 2, whereas those for the **M2** and **O2** assemblies are shown in Figure 3. The voltammogram of the **T1** assembly (not shown) is similar to that of the **D1** assembly. The general voltammetric charac-

Table 1. Redox Potentials (V) of the TD SAMs^a

TD	$E^{0/+}$	$E^{+/2+}$	$E^{2+/3+}$	$E^{3+/4+}$
M1	0.24	0.68	1.13	1.34
D1	0.30	0.77	1.23	1.44
T1	0.31	0.76	1.23	1.48
M2	0.27	0.72	1.18	1.39
O2	0.52	0.99	1.46	1.68

^a SAM potentials were obtained in CH_2Cl_2 containing $1.0 \text{ M } n\text{-Bu}_4\text{NPF}_6$. E -values vs Ag/Ag^+ ; scan rate = 100 V s^{-1} . The solution potentials for the five TDs (obtained in CH_2Cl_2 containing $0.1 \text{ M } n\text{-Bu}_4\text{NPF}_6$) are identical and are as follows: $E^{0/+} \sim 0.22 \text{ V}$; $E^{+/2+} \sim 0.57 \text{ V}$; $E^{2+/3+} \sim 1.08 \text{ V}$; $E^{3+/4+} \sim 1.29 \text{ V}$. E -values vs Ag/Ag^+ ; $\text{FeCp}_2/\text{FeCp}_2^+ = 0.19 \text{ V}$; scan rate = 0.1 V s^{-1} . Values are $\pm 0.03 \text{ V}$.

Table 2. Charge Densities and Molecular Packing Characteristics of the TD SAMs

TD	σ_0 ($\mu\text{C cm}^{-2}$)	Γ_0^a ($10^{-11} \text{ mol cm}^{-2}$)	molecular area ^a (\AA^2)	thickness (\AA)
M1	2.4	2.5	670	13
D1	9.3	9.6	170	24
T1	3.4	3.5	470	14
M2	1.5	1.6	1070	16
O2	2.6	2.7	620	26

^a The values for the oligomers are effective values because they are not normalized for the number of redox equivalents per molecule (see text).

teristics of the TD assemblies are totally consistent with the formation of relatively homogeneous SAMs wherein the complexes are tethered to Au via thiol linker(s). It should be noted that noncovalently attached deposits on the electrode (as opposed to SAMs) do not give well-resolved voltammetric peaks. In addition, deposits that are not covalently anchored to the surface readily wash off during the sonication and rinsing processes used in the preparation of the samples.

The general voltammetric characteristics of the SAMs of the different TDs are similar to one another; however, the detailed appearance and exact potentials of the redox waves are different. Other general features of the voltammetric behavior include the following: (1) Studies wherein the deposition time was increased from tens of minutes to hours did not result in any further increase in current. Accordingly, the voltammograms shown are the most densely packed SAMs that can be easily obtained for the TD complexes. (2) The anodic and cathodic peak positions for all of the TD SAMs are independent of scan rate, and the E_{fwhm} is in the $0.10\text{--}0.15 \text{ V}$ range for each redox couple. (3) The voltammetric characteristics of all of the TD SAMs do not change appreciably upon repeated (> 50 scans) redox cycling under ambient conditions.

The redox potentials of all five TD SAMs are summarized in Table 1. The charge densities (σ_0) obtained by integrating the voltammetric waves are summarized in Table 2. The surface concentrations (Γ_0) and molecular areas (\AA^2) calculated from the charge densities are also included in the table. The calculated surface concentrations and molecular areas for the oligomers are not normalized to account for the fact that each redox wave represents a multielectron process. Therefore, these values represent effective surface concentrations and molecular areas. The true values depend on the details of the molecular orientation of the redox centers with

respect to the surface (vide infra). There are several noteworthy features in the voltammetric behavior of the TDs.

(1) The formal potential for each of the waves of all of the TDs in the SAMs are more positive than those observed in solution. The positive shift of the formal potential in the SAM versus solution is consistent with previous studies of ferrocene- and porphyrin-containing SAMs on Au.^{1,3–5,8,17–21} The magnitudes of the positive shifts are generally similar for the **M1**, **D1**, **T1**, and **M2** SAMs and are less than 0.2 V. The **O2** SAM is the exception. The potential shifts for the SAM of this oligomer are significantly larger than those of the other TDs, ranging from 0.3 to 0.4 V. The different voltammetric behavior observed for the **O2** SAM cannot be attributed solely to the nature of the linker to the surface (diphenylbutadiyne versus diphenylethyne) because **M2**, which contains the same linker, exhibits behavior similar to the TDs which contain diphenylethyne linkers.

(2) The charge densities for the SAMs of TDs with diphenylethyne linkers are generally larger than those of the TDs with diphenylbutadiyne linkers. In addition, for SAMs with the same type of linker, the charge densities of the oligomers are higher than for the monomers. Qualitatively, these results indicate that diphenylethyne linkers yield more tightly packed TD SAMs than diphenylbutadiyne linkers and that oligomers can be more tightly packed than monomers. A more interesting characteristic of the molecular packing emerges upon inspection of the calculated effective surface concentrations and molecular areas. In particular, the effective surface concentrations and molecular areas for the **M1**, **T1**, and **O2** TD SAMs are generally quite similar to one another, with the effective molecular areas falling in the 500–700 Å² range. These molecular areas are larger than would be expected for a tightly packed monolayer of monomeric TDs, whose molecular footprint is in the 200–400 Å² range, depending on the exact orientation of the molecule with respect to the surface and how the tether contributes to the footprint. In contrast, the effective molecular area of the **D1** SAM is ~170 Å², which is close to the smallest possible molecular footprint of a monomeric TD. The molecular area for the **M2** SAM is ~1070 Å², which is much larger than that for any of the other TDs.

Ellipsometric Characteristics of the TD SAMs. To gain additional information on the orientation of the TDs in the SAM, the thickness of the various SAMs was evaluated using ellipsometry. The values obtained for the SAM thickness of the five TDs are included in Table 2. Inspection of these data reveals that the **M1**, **T1**, and **M2** SAMs are comparable in thickness (~14 Å), whereas the **D1** and **O2** SAMs are somewhat thicker (~25 Å). The measured thickness for all the TD SAMs is significantly less than the end-to-end dimensions of any of the molecules. Recall that the length of the **M1** complex is ~35 Å, whereas the **T1** complex is ~72 Å. The **O2** complex is even longer; however, its length cannot be defined exactly because it is a mixture of oligomers. On the other hand, dimensions of ~25 Å (or less) are qualitatively comparable to the height of a TD stack (with the planes of the macrocycles parallel to the surface).

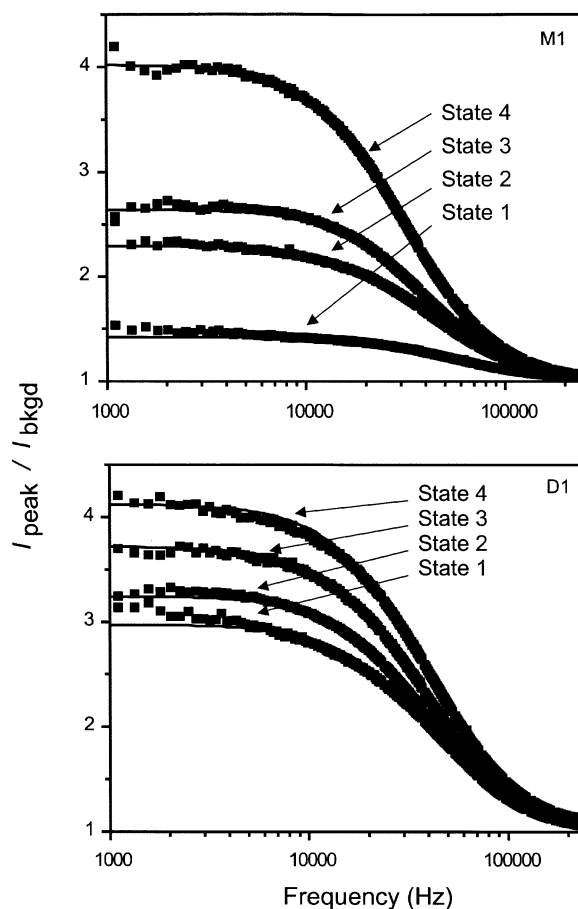


Figure 4. $I_{\text{peak}}/I_{\text{bkgd}}$ (squares) versus frequency for the mono-, di-, tri-, and tetracations (from smallest-to-large ratio) of the **M1** and **D1** SAMs. The solid lines are fits to the data using a Randles equivalent circuit. The fitting parameters are as follows. **M1**: $\Gamma \sim 2.0 \times 10^{-12}$ mol cm⁻²; state 1, $k^0 \sim 160 \times 10^3$ s⁻¹; state 2, $k^0 \sim 107 \times 10^3$ s⁻¹; state 3, $k^0 \sim 98 \times 10^3$ s⁻¹; state 4, $k^0 \sim 73 \times 10^3$ s⁻¹. **D1**: $\Gamma \sim 1.5 \times 10^{-12}$ mol cm⁻²; state 1, $k^0 \sim 97 \times 10^3$ s⁻¹; state 2, $k^0 \sim 87 \times 10^3$ s⁻¹; state 3, $k^0 \sim 85 \times 10^3$ s⁻¹; state 4, $k^0 \sim 80 \times 10^3$ s⁻¹.

Electron-Transfer Characteristics of the TD SAMs. The standard electron-transfer rate constants (k^0) were measured for each redox state of the five TD SAMs using swept waveform ac voltammetry (SWAV). A detailed description of the method, the data analysis procedure, and the relation of k^0 to the measured parameters (the ratio of the peak current to the background current ($I_{\text{peak}}/I_{\text{bkgd}}$) as a function of frequency) have been reported elsewhere.⁴ Previous studies of other types of porphyrin SAMs have shown that the k^0 values are particularly sensitive to the surface concentration when the concentration falls in the range $\Gamma \sim 1 \times 10^{-11}$ to 3×10^{-11} mol cm⁻².⁴ In this range, the electron-transfer rates fall by 1 order of magnitude as the surface concentration increases. Consequently, the surface concentrations of the TDs were maintained below 1×10^{-11} mol cm⁻² for the measurement of the electron-transfer rates. Identical surface concentrations could not be obtained for the five different TD SAMs; accordingly, some differences in rates may be due to surface coverage effects. However, these effects should not affect the rates by more than a factor of 2.

Representative plots of $I_{\text{peak}}/I_{\text{bkgd}}$ for the **M1** and **D1** SAMs are shown in Figure 4; plots for the **M2** and **O2** SAMs are

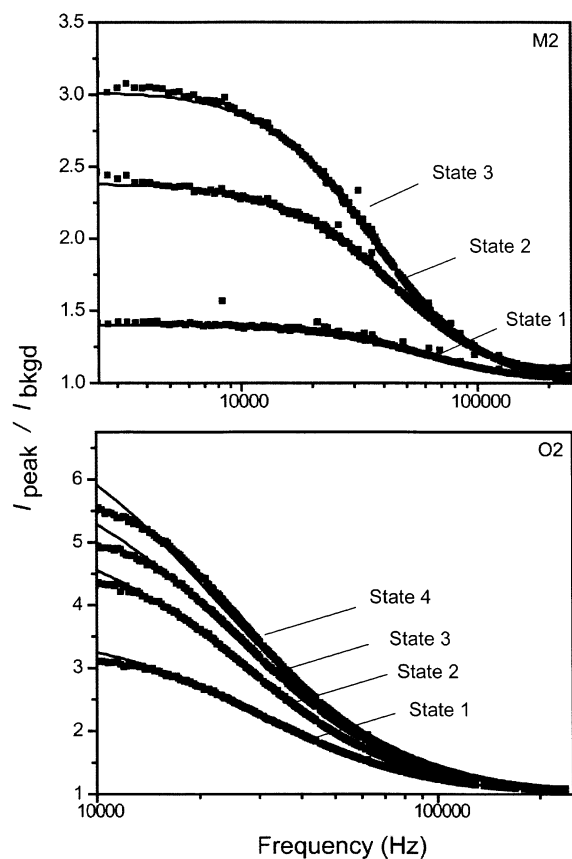


Figure 5. $I_{\text{peak}}/I_{\text{bkgd}}$ (squares) versus frequency for the mono-, di-, tri-, and tetracations (from smallest-to-large ratio) of the **M1** and **D1** SAMs. The solid lines are fits to the data using a Randles equivalent circuit. The fitting parameters are as follows. **M2**: $\Gamma \sim 3.1 \times 10^{-12}$ mol cm $^{-2}$; state 1, $k^0 \sim 174 \times 10^3$ s $^{-1}$; state 2, $k^0 \sim 110 \times 10^3$ s $^{-1}$; state 3, $k^0 \sim 86 \times 10^3$ s $^{-1}$; state 4, k^0 could not be determined accurately owing to the presence of a large background current. **O2**: $\Gamma \sim 5.4 \times 10^{-12}$ mol cm $^{-2}$; state 1, $k^0 \sim 70 \times 10^3$ s $^{-1}$; state 2, $k^0 \sim 58 \times 10^3$ s $^{-1}$; state 3, $k^0 \sim 54 \times 10^3$ s $^{-1}$; state 4, $k^0 \sim 45 \times 10^3$ s $^{-1}$.

shown in Figure 5. The data for I_{peak} were collected at $E^{n+/(n+1)+}$; the data I_{bkgd} were collected 0.14 V below $E^{n+/(n+1)+}$. The k^0 values obtained from the fits of the plots of $I_{\text{peak}}/I_{\text{bkgd}}$ versus frequency are summarized in Table 3. Inspection of the kinetic data reveals the following trends: (1) The electron-transfer rates of all of the TD SAMs monotonically decrease with increasing oxidation state. This behavior is consistent with that we have previously observed for monothio-derivatized TD SAMs.⁴ (2) The electron-transfer rates for the SAMs of TDs with diphenylethyne linkers are generally comparable to those of the TDs with diphenylbutadiyne linkers. Furthermore, the k^0 values for all five TDs are arguably similar to one another considering the possible effects of surface concentration on the exact k^0 values. (3) The electron-transfer rates for all the dithio-derivatized TD SAMs studied herein are generally faster (~ 3 -fold) than those of monothio-derivatized TD SAMs (all of which were monomers) that we have previously investigated.⁴

Charge-Retention Characteristics of the TD SAMs. The charge-retention characteristics of the TD SAMs were investigated in parallel with the electron-transfer kinetics. These measurements were made on the same SAMs used

for the electron-transfer studies described above. The charge-dissipation rates were measured using open circuit potential amperometry (OCPA). A detailed description of the method and the data analysis procedure has been reported elsewhere.³ In previous studies of charge retention of porphyrin and other TD SAMs, we have found that charge-dissipation rates follow approximately first-order kinetics;^{1,2,4,5} thus, we have characterized these rates in terms of a charge-retention half-life ($t_{1/2}$).

Representative charge-retention data sets are shown for the **D1** and **O2** SAMs in Figures 6 and 7, respectively. The top panel in each figure shows the current-decay transients of the four different oxidized states to the neutral state ($E_n \rightarrow E_0$, $n = 1-4$). The four traces shown for each state are the reductive current measured from the oxidized SAMs after selected disconnect times (15, 30, 60, and 80 s) followed by reconnection at the open circuit potential (wherein molecules that have remained oxidized are reduced). The bottom panel in each figure shows the integrated current-decay transients for the four different oxidized states. The four traces shown are for the 30 s traces shown in each of the four frames in the top panel. The integrated current data were fit to a first-order rate law ($r^2 > 0.98$) to determine the $t_{1/2}$ values, which are included in Table 3.

Inspection of the data shown in Table 3 reveals that the charge-retention characteristics of the TD SAMs parallel the electron-transfer characteristics. In particular, the data reveal the following features: (1) The charge-retention times of all of the TD SAMs monotonically increase with increasing oxidation state. This behavior is consistent with that we have previously observed for monothio-derivatized TD SAMs.^{4,5} (2) The charge-retention times for the SAMs of TDs with diphenylethyne linkers are generally comparable to those of the TDs with diphenylbutadiyne linkers. Furthermore, the $t_{1/2}$ values for all five TDs are arguably similar to one another considering the possible effects of surface concentration on the exact $t_{1/2}$ value. (3) The charge-retention times of all the dithio-derivatized TD SAMs studied herein are generally shorter (~ 3 -fold) than those of monothio-derivatized TD SAMs (all of which were monomers) that we have previously investigated.^{4,5}

Discussion

The studies reported herein indicate that the bis(*S*-acetylthio)-derivatized TDs form stable SAMs that exhibit robust, reversible electrochemical behavior. These SAMs also exhibit desirable features for potential use as molecular capacitors in memory cells, in particular, charge-retention times on the orders of tens of seconds. Many of the general characteristics of the redox, electron-transfer, and charge-retention behavior of the dithio-derivatized TDs are similar to those we have previously discussed for monothio-derivatized analogues;^{4,5,8} the reader is referred to these earlier publications for a more detailed discussion of these properties of the SAMs. Here, we focus on more general aspects of the properties of the dithio-derivatized TD SAMs and on particular features that distinguish the behavior of these SAMs from those of monothio-derivatized analogues.

Table 3. Electron-Transfer Rates (k^0) and Charge-Retention Half-Lives ($t_{1/2}$) of the TD SAMs^a

TD	state 1		state 2		state 3		state 4	
	k^0 (10^3 s^{-1})	$t_{1/2}$ (s)	k^0 (10^3 s^{-1})	$t_{1/2}$ (s)	k^0 (10^3 s^{-1})	$t_{1/2}$ (s)	k^0 (10^3 s^{-1})	$t_{1/2}$ (s)
M1	160	14	107	27	98	36	73	38
D1	97	19	87	20	85	24	80	28
T1	100	16	85	23	79	40	54	43
M2	174	9	110	14	86	24	b	36
O2	70	20	58	29	54	39	45	53

^a The effective surface concentrations of the SAMs were the following: **M1**, $\Gamma \sim 2.0 \times 10^{-12} \text{ mol cm}^{-2}$; **D1**, $\Gamma \sim 1.5 \times 10^{-12} \text{ mol cm}^{-2}$; **T1**, $\Gamma \sim 1.0 \times 10^{-11} \text{ mol cm}^{-2}$; **M2**, $\Gamma \sim 3.1 \times 10^{-12} \text{ mol cm}^{-2}$; **O2**, $\Gamma \sim 5.4 \times 10^{-12} \text{ mol cm}^{-2}$. ^b k^0 could not be obtained owing to the presence of a large background current.

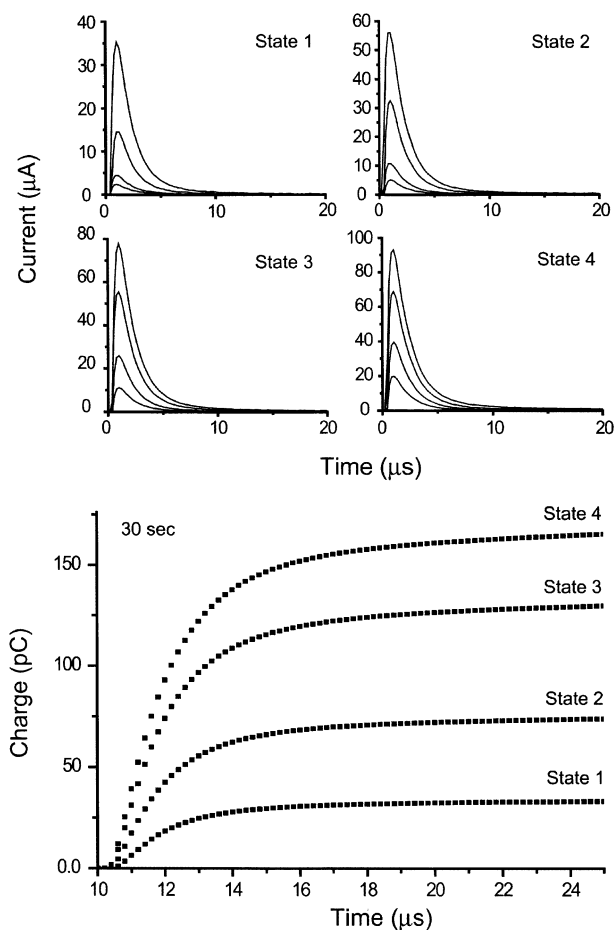


Figure 6. Current-decay transients for the **D1** SAM. Top panel: Charge decay of the four different oxidized states to the neutral state ($E_n \rightarrow E_0$, $n = 1-4$). The four traces shown for each state are the reductive current measured at 15, 30, 60, and 80 s after disconnection from the source of applied potential. Bottom panel: Integrated current-decay transients for the four different oxidized states. The four traces shown are for the 30 s traces shown in each of the four frames in the top panel.

One general theme that emerges from the present studies is that the diphenylethyne linker affords more densely packed SAMs than does the diphenylbutadiyne linker. This behavior could be explained by the fact that the former linker is shorter and more rigid (with respect to both torsional and angular deformations) than the latter. The ethyne unit is stiff in a linear direction but subject to considerable bending, owing to the sp-hybridization of the ethyne carbons. Indeed, 1,4-diphenylethyne and 1,4-diphenylbutadiyne linkers attached to porphyrins give average bending of 26 and 31°, respectively.⁴¹ The decreased deformations associated with the

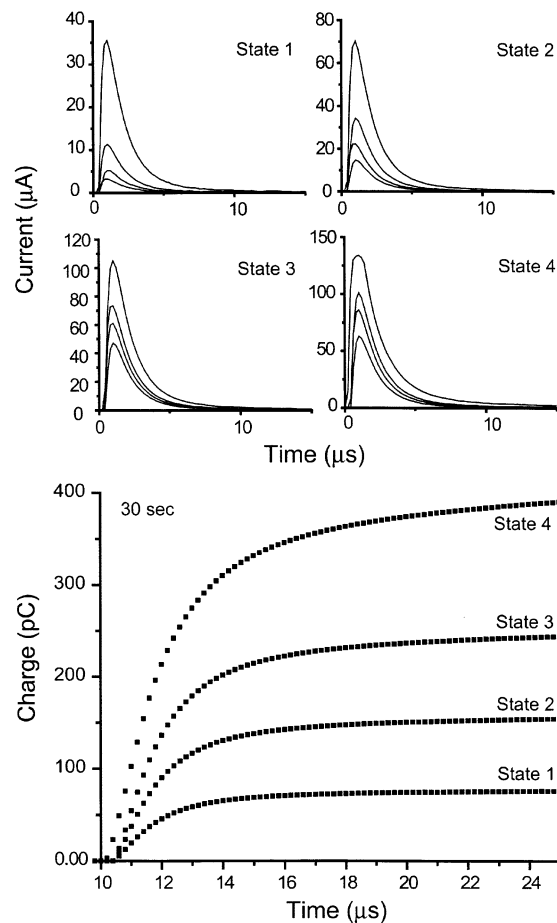


Figure 7. Current-decay transients for the **O2** SAM. Top panel: Charge decay of the four different oxidized states to the neutral state ($E_n \rightarrow E_0$, $n = 1-4$). The four traces shown for each state are the reductive current measured at 30, 60, 80, and 100 s after disconnection from the source of applied potential. Bottom panel: Integrated current-decay transients for the four different oxidized states. The four traces shown are for the 30 s traces shown in each of the four frames in the top panel.

diphenylethyne linker would mitigate both the enthalpic and entropic penalty associated with constraining these motions in a more tightly packed SAM. A second general theme is that the oligomeric TDs form more tightly packed SAMs than do the monomeric TDs. The behavior could be explained by the natural tendency of extended linear architectures to arrange in two-dimensionally ordered patterns. A third general theme is that the dithio-derivatized TDs exhibit generally faster electron-transfer and charge-dissipation rates

(41) Bothner-By, A. A.; Dadok, J.; Johnson, T. E.; Lindsey, J. S. *J. Phys. Chem.* **1996**, *100*, 17551–17557.

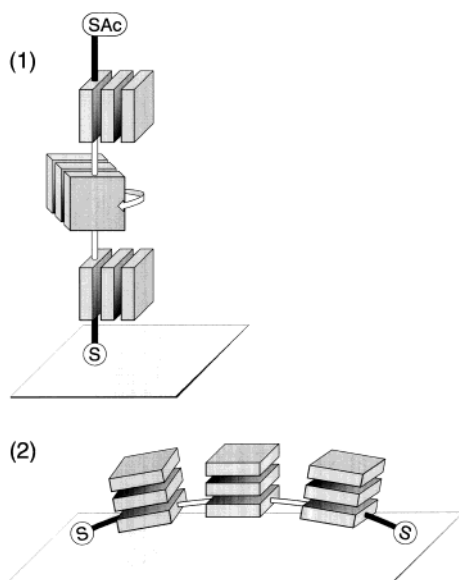


Figure 8. Two distinct surface orientations of the TD triad **T1**: (1) vertical orientation upon attachment via one thio group, enabling free rotation of the TDs about the linear axis; (2) supine orientation upon attachment via two thio groups. Slight bowing of the molecular architecture occurs owing to bending of the four diphenylethyne linkers.

than do monothio-derivatized analogues. This observation suggests that the geometry of dithio-derivatized TDs on the surface is fundamentally different from that of monothio-derivatized TDs. The key question is what is the exact nature of these differences?

The detailed molecular geometry of the monothio-derivatized TD SAMs has not been determined. However, the measured molecular areas of these TDs are generally consistent with the aryl-alkyne linkers adopting an orientation that is closer to surface normal rather than one that is significantly tilted.^{5,8} In this geometry, the planes of the macrocycles of the TD are approximately perpendicular to the plane of the surface. The dithio-derivatized TDs could also adopt a similar geometry, which would require that attachment to the surface occurs via only one of the two thiols. On the other hand, the dithio-derivatized TDs could orient with their tethers/backbones approximately parallel to the plane of the surface. In this geometry, the planes of the macrocycles in the TDs would also be more parallel to the plane of the surface (like a stack of coins) and attachment could potentially occur via both thiols (Figure 8). The experimental data reported herein for the dithio-derivatized TD SAMs are most consistent with the latter surface geometry. However, we emphasize that even if the horizontal geometry is preferred, we have no direct experimental evidence that the second thiol attaches to the Au surface. These issues will be discussed in more detail below.

The elucidation of the surface geometry of the monomeric TDs from the data at hand is more difficult than for the oligomeric TDs. In particular, the molecular areas of both the **M1** ($\sim 670 \text{ \AA}^2$) and **M2** ($\sim 1070 \text{ \AA}^2$) SAMs are larger than the molecular footprint of a TD. Accordingly, the molecules could be relatively sparse on the surface with their tethers parallel, perpendicular, or tilted with respect to the surface. The principal evidence that the complexes are

oriented with their tethers and the planes of the macrocycles in the TD more parallel to the surface derives from the measured SAM thickness and the electron-transfer/charge-dissipation rates. As noted above, the thickness of the SAMs is much smaller than the end-to-end length of the complexes. However, interpretation of these data is somewhat complicated by the fact that molecules are relatively sparse on the surface and the measured thickness must reflect an average of covered and noncovered area. The measured thickness would necessarily be less than the actual thickness of the SAM owing to the regions of bare surface. The kinetic data are perhaps a better indicator of a parallel geometry. In particular, both the electron-transfer and charge-dissipation rates for the dithio-derivatized TDs are significantly faster than those of monothio-derivatized analogues. A more parallel surface geometry for the former TDs would be expected to give rise to faster rates because this geometry places the π -electron density of the TD much closer to the surface, which in turn could promote direct electron transfer to the surface (rather than through the linker group). Faster apparent rates would also be expected if the TDs are indeed attached via two thiols. This follows because the presence of two connections to the surface provides an additional through-linker electron-transfer pathway. The presence of two equivalent pathways results in an apparent rate for any kinetic process that is twice that for a single pathway (even though the intrinsic rates along a given pathway are the same).

The experimental data for the oligomeric SAMs are more compelling for a parallel surface geometry. The oligomeric TDs exhibit generally smaller surface areas (**D1** $\sim 170 \text{ \AA}^2$; **T1** $\sim 470 \text{ \AA}^2$; **O2** $\sim 620 \text{ \AA}^2$) than the monomeric TDs (**M1** $\sim 670 \text{ \AA}^2$; **M2** $\sim 1100 \text{ \AA}^2$) and thicknesses that are comparable (**M1**, **M2**, and **T1** $\sim 15 \text{ \AA}$) or only slightly larger (**D1** and **O2** $\sim 26 \text{ \AA}$). The measured thicknesses of the oligomers, particularly the **T1** and **O2** SAMs, are totally incompatible with a vertical orientation of the oligomer backbone with respect to the plane of the surface (even if the presence of some open space results in an average thickness that is less than that of the molecular component). The measured molecular areas are also generally inconsistent with a vertical geometry; however, the argument is more subtle. In particular, if the oligomeric TDs were in a vertical orientation, their effective molecular area would be scaled to smaller values than the actual molecular footprint because the charge density would increase linearly with the number of equivalent redox centers. Thus, a vertical orientation for the **T1** or the **O2** SAM (which have ≈ 3 equivalent redox centers) would result in an effective area that is much smaller than that of a monomer. In contrast, a horizontal backbone orientation on the surface would result in a similar charge density for an oligomer and monomer and, hence, a similar molecular area. While the molecular areas for the **T1** and **O2** SAMs are somewhat smaller than those of the monomers, they are not radically smaller, as would be expected if three (or more) redox centers were vertically stacked. The fact that the electron-transfer and charge-dissipation rates for the oligomeric TD SAMs are comparable to one another and

comparable to those of the monomers further argues for a similar orientation for all of the TD SAMs.

Finally, we note that there are certain unexplained aspects of the surface packing characteristics of the TD SAMs. The behavior of the **D1** SAM is the most unusual. This oligomer appears to pack much better than the other TDs, as is evidenced by its near limiting molecular area. The more dense arrangement of the **D1** SAM could also be responsible for the fact that the measured thickness is nearly twice that of the **M1**, **M2**, or **T1** SAMs (hence there is less open space on the surface to reduce the apparent thickness). We also note that the concept of a completely vertical or horizontal orientation is likely an oversimplification. As was noted above, we have no direct evidence that the dithio-derivatized TDs are attached via both thiols (albeit the circumstantial evidence is significant). For any species attached via a single thiol there would most likely be a distribution of tilt angles with respect to the surface. Even if the TDs are attached via two thiols, the butadiyne moiety, which serves both as a linker to the surface and the connecting group between constituents in the oligomers, is sufficiently flexible that a long dithio-attached oligomer could bow off the surface (Figure 8). In oligomers such as **T1** or **O2**, whose end-to-end lengths are 70 Å or more, a bow angle of 10° would significantly elevate a TD constituent in the middle of the rod relative to a TD constituent at the end of the rod.

Summary and Conclusions

A series of bis(*S*-acetylthio)-derivatized TD complexes of general form AcS-(TD)_{*n*}-SAc (*n* = 1–3) has been synthesized by Pd-catalyzed coupling (Sonogashira- or Glaser-type) of TD building blocks. Pd-catalyzed Glaser couplings of a bis(ethynylphenyl) TD monomer afforded TD oligomers with a large number of repeat units (*n* > 10). The large oligomers are soluble in common organic solvents (e.g., ~5 mg/mL of CHCl₃), which enables processing in solution.

All of the bis(*S*-acetylthio)-derivatized TD complexes readily form SAMs on Au that exhibit robust, reversible electrochemical behavior. Four well-resolved anodic waves representing the mono-, di-, tri-, and tetracation radicals are observed within the potential range of (0–1.6 V) for all SAMs. The electron-transfer rates for the various states of all of the TD SAMs are similar to one another and are in the 10⁴–10⁵ s⁻¹ range. The charge retention half-lives are also similar and are in the 10–60 s range. Collectively, the body of electrochemical and ellipsometric data are most consistent with the TDs being oriented in an approximately parallel fashion with respect to the plane of the surface. This orientation would permit attachment via both thiols.

The general characteristics of the TD SAMs, particularly the oligomers, indicate that these complexes have a number of properties that would render these complexes good candidates for use in molecular capacitors. In particular, the TD SAMs are relatively stable, which affords robust electrochemical cycling (equivalent to read/write operations) and facilitates detection of stored charge (due to increased capacitance). The TD SAMs also retain charge for tens of seconds, which is significantly longer than the millisecond

charge-retention times of current semiconductor-based trench capacitors that are used in modern dynamic random access memories.

Experimental Section

Full synthetic procedures and characterization data for all new compounds are provided in the Supporting Information.

Square-Wave Voltammetry. The solution voltammetric characteristics of the TDs were investigated with square-wave methods using procedures and instrumentation previously described.⁵ The electrolyte solution was 1.0 M *n*-Bu₄NPF₆ (recrystallized three times from methanol and dried under vacuum at 110 °C) in anhydrous CH₂Cl₂. This solvent/electrolyte system was also used for the SAM electrochemical experiments described below. The potentials were measured vs Ag/Ag⁺; $E_{1/2}(\text{FeCp}_2/\text{FeCp}_2^+) = 0.19 \text{ V}$ at scan rate of 0.1 V s⁻¹.

Cyclic Voltammetry. The SAM voltammetric characteristics of the TDs were investigated with fast-scan cyclic methods using a Gamry Instruments PC4-FAS1 femtostat running PHE200 Framework and Echem Analyst software. The voltammetry of the SAMs was recorded in three-electrode mode. The electrodes were prepared as follows: (1) The working electrode was an Au ball constructed from a 25 μm diameter Au wire (Alpha Aesar, 99.9%) sealed in soft glass. Initially a ~750 μm segment of the Au wire protruded from the end of a 1 mm i.d. soft glass capillary. Exposure of the glass capillary to a flame melted the glass, which formed a tight seal around the Au. The exposed wire retracted and melted into a ball that terminated at the surface of the sealed glass during this process. The electrode was then immediately cooled in a stream of nitrogen (99.999%) and immersed in a ~2 mg/mL CH₂Cl₂ solution of the TD for 10 min. The electrode was then removed from the solution, thoroughly rinsed 3 times with CH₂Cl₂, and immediately inserted into the electrolyte solution. (2) The reference electrode was a 0.5 mm diameter Ag wire precleaned by sonicating in NH₄OH solution (36%, Fisher) for 10 min, followed by a purified water rinse and then an acetone (HPLC grade, Fisher) rinse. (3) The counter electrode was a Pt wire. The electrochemical area of the Au ball working electrode (which was used to evaluate the SAM surface concentration) was evaluated by measuring the anodic peak current from a 1 mM ferrocene solution and applying the Randles–Sevcik equation.⁴²

Swept Waveform AC Voltammetry (SWAV). The electron-transfer characteristics of the TD SAMs were investigated using SWAV techniques according to methods previously described.⁴ The Au working and Ag reference electrodes and the SAMs were prepared as described above. The only difference was that a 5 μm Au wire was used to prepare the working electrode. The smaller electrode was used to ensure a fast RC response (≤5 μs) of the electrochemical cell. Briefly, the SWAV experiment is performed as follows. The potential is set at the $E_{1/2}$ value of a particular oxidation state of the SAM, and the frequency of the applied waveform is swept in time while maintaining a constant amplitude.⁴ A background is then collected by repeating the experiment with the applied potential 140 mV below the $E_{1/2}$ value. The time-domain current response obtained at the formal potential is then ratioed to that collected at the background potential, and the data are Fourier transformed to obtain a current ratio vs frequency plot. The k^0 values were obtained by fitting the plots using an Excel spreadsheet program (provided by S. E. Creager).

(42) Bard, A. J.; Faulkner, L. R. *Electrochemical Methods: Fundamentals and Applications*; Wiley: New York, 2001.

Open Circuit Potential Amperometry (OCPA). The charge-retention characteristics of the TD SAMs were evaluated using OCPA techniques according to methods previously described.^{1–3} The OCPA measurements were made using the same electrochemical cell described above for the SWAV experiments. Briefly, the OCPA experiment is performed as follows. (1) The SAM is oxidized with a 20 ms pulse ~ 100 mV above the formal potential of the desired redox state. This pulse length is longer than the RC constant of the cell which precludes the cell response interfering with the measurements. (2) The applied potential is disconnected at the counter/reference electrode for a variable period of time.³ During this disconnect time period, the electrochemical cell relaxes to the open circuit potential (OCP), after which the applied potential is changed to match the OCP. (3) The counter electrode is then reconnected, and the resulting current is monitored as the SAM is reduced (because the OCP is at a reducing potential). The magnitude of the observed current is proportional to the number of molecules in the SAM that remain oxidized while the counter/reference electrode is disconnected. Charge retention is measured by successively changing the disconnect time up to a point where all of the molecules have decayed back to the neutral state.

Ellipsometry. The effective layer thickness of each TD SAM was measured using a Gaertner L 116B ellipsometer running Gaertner software for all serial calculations (GEMP). The light source was the monochromatic polarized beam from a He–Ne laser ($\lambda = 632$ nm) adjusted with a 90° quarter-wave compensator. All measurements were performed with both the polarizer and analyzer positioned such that the angles of incidence and reflection were 70° with respect to the normal of the plane of the substrate containing the SAM. The substrate was prepared by evaporating Au (99.99%) onto a cleaned thermally oxidized undoped Si wafer using a Sloan E-Beam evaporator. Prior to Au deposition, a 100 \AA

Cr underlayer was evaporated to promote better adhesion of the Au to the oxidized Si. The Au was evaporated at a rate of $\sim 1.5 \text{ \AA/s}$ at a chamber pressure of 1×10^{-7} Torr. The Au film thickness was measured to be $\sim 2000 \text{ \AA}$ by using a QCM sensor, consistent with the value of 2030 \AA measured ellipsometrically (using the optical parameters for Au: $n = 0.09$; $k = 3.473$).⁴³ Following this process, the Au films were immediately cut into 1 cm^2 pieces and immersed for 15 min in an ~ 2 mM solution of the TD in CH_2Cl_2 . Each piece was immediately rinsed in neat CH_2Cl_2 , sealed in a gastight vial and purged dry with Ar. Samples were stored under Ar for at most a few hours prior to the ellipsometric measurements. The thickness of the TD SAMs was calculated assuming that $n = 1.45$. Each sample was measured at five different locations within the 1 cm^2 surface area to determine the spatial deviation in the thickness of the monolayers. In all cases, the measured deviation in five successive measurements was $< 5\%$.

Acknowledgment. This work was supported by the DARPA Moletronics Programs (Grant MDA972-01-C-0072) and by ZettaCore, Inc. Mass spectra were obtained at the Mass Spectrometry Laboratory for Biotechnology at North Carolina State University. Partial funding for the facility was obtained from the North Carolina Biotechnology Center and the NSF.

Supporting Information Available: Complete experimental section, including mass and ^1H NMR spectra for each new compound. This material is available free of charge via the Internet at <http://pubs.acs.org>.

IC034730U

(43) Nielsen, M.; Larsen, N. B.; Gothelf, K. V. *Langmuir* **2002**, *18*, 2795–2799.